Theoretical Evaluation of the Effect of Internal Heat Exchanger in Standard Vapor Compression and Compressor-Driven Ejector Refrigeration Systems

John Carlo S. Garcia and Menandro S. Berana

***Abstract*— This paper provides a theoretical analysis on the effect of internal heat exchanger (IHX) on a system using standard vapor compression cycle (VCC) and compressor-driven ejector refrigeration cycle (CDERC). The CDERC has a nozzle and a supersonic diffuser which is used to avoid formation of shock along the mixing section of the ejector. Parameters such as the degree of subcooling of the refrigerant at the condenser exit and the heat transfer ratio (HTR) in the IHX are varied while the condensing and evaporating temperatures are held constant. It is found out that the increase in the degree of subcooling in CDERC with IHX increases the entrainment ratio and lowers the separator temperature. The utilization of IHX in VCC and CDERC is applicable only with lower values of degree of subcooling and HTR from the view of the systems' coefficient of performance (COP).**

This paper also presents the performance of ammonia, R22, R134a and propane in the two systems. It is seen that propane performs satisfactorily in both VCC and CDERC with IHX, while R134a is seen to only perform well in VCC with IHX.

The IHX does not necessarily improve the performance of compressor-driven refrigeration systems. It mainly functions as a safeguard to ensure that the fluid that enters the compressor is in vapor form. In some cases, as seen in standard VCC using R134a, improving the COP by adding an IHX becomes an added advantage.

***Index Terms*— ejector, internal heat exchanger, refrigeration, coefficient of performance**

I. Introduction

Refrigeration is defined as the process of removing heat from a lower temperature reservoir (refrigerated space) and transferring it to a higher temperature reservoir, usually to the surroundings. It is usually done through mechanical means via the standard vapor compression cycle (VCC) [1].

Manuscript received March 6, 2017; revised April 17, 2017. The dissemination of this research is sponsored by the Engineering Research and Development Program (ERDT) of the Department of Science and Technology (DOST) of the Republic of the Philippines. The program is being managed and implemented by the College of Engineering of University of the Philippines–Diliman.

J. C. S. Garcia is an instructor of the Department of Mechanical Engineering, College of Engineering, University of the Philippines – Diliman, Quezon City, 1101 Philippines (phone: +63-917-717-3110, +63-2-981-8500 loc 3130; fax: +63-2-920-8860; e-mail: jsgarcia1@up.edu.ph).

M. S. Berana is an associate professor of the Department of Mechanical Engineering, College of Engineering, University of the Philippines – Diliman, Quezon City, 1101 Philippines (phone: +63-915-412-0022, +63-2-981-8500 loc 3130; fax: +63-2-920-8860; e-mail: menandro.berana@coe.upd.edu.ph).

A. Compressor-Driven Ejector Refrigeration Cycle

One of the modifications in the standard VCC, and also an emerging technology, is the use of an ejector. The ejector is utilized either as a compressor or as an expansion device in two of its configurations: compressor-driven [2] and heat-driven. This technology is becoming more attractive because it improves the system's performance by minimizing the compression work and throttling losses.

The compressor-driven ejector refrigeration cycle (CDERC), as shown in schematic and P-h diagrams in Fig. 1 and Fig. 2, respectively, has two refrigerant flows: the primary and secondary flows. In the primary flow, the refrigerant is circulated by the compressor in the condenser, ejector, and separator. Meanwhile, the refrigerant is circulated in the expansion device, evaporator, ejector, and separator in the secondary flow.

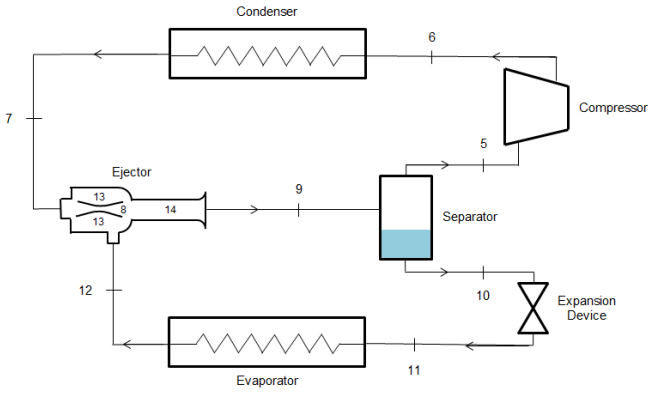

Fig. 1. Schematic diagram of the CDERC

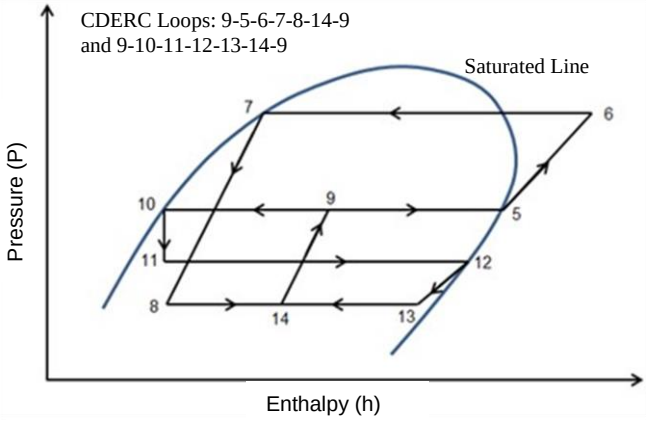

Fig. 2. P-h diagram of the CDERC

ISBN: 978-988-14048-3-1
ISSN: 2078-0958 (Print); ISSN: 2078-0966 (Online)

As also shown in Fig. 1 and Fig. 2, the refrigerant, at its saturated vapor state (state 5), enters the compressor and exits at the condenser pressure (state 6). The refrigerant is then cooled at the condenser (state 7) by rejecting heat to the surrounding medium. The refrigerant enters the ejector as the primary fluid (state 8), where it entrains in vapor from the evaporator (state 13). It is then diffused in the diffuser where it recovers pressure (state 9). The refrigerant that exits the ejector is separated into saturated vapor (state 5) and saturated liquid (state 10) in the vapor-liquid separator. The saturated vapor returns to the compressor while the saturated liquid is then throttled in an expansion device. The pressure drops as the fluid exits the expansion device (state 11), and the refrigerant enters the evaporator. It then vaporizes (state 12) as heat is transferred from the refrigerated space. The saturated vapor returns to the ejector as the secondary fluid (state 13).

When compared to a standard VCC, the suction pressure of CDERC is higher. This results in a lower compression work, thus, also having a higher COP.

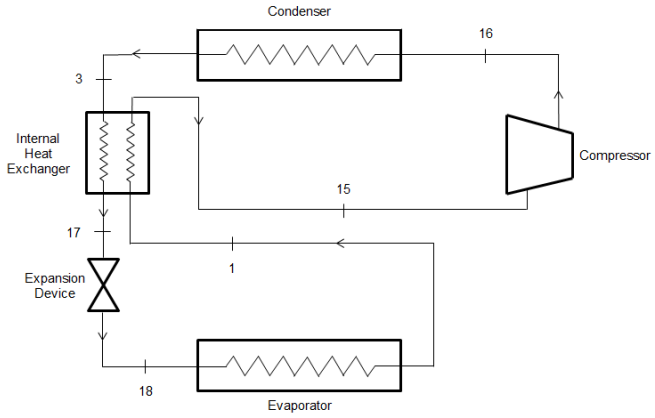

Fig. 3. Schematic diagram of the standard VCC with IHX

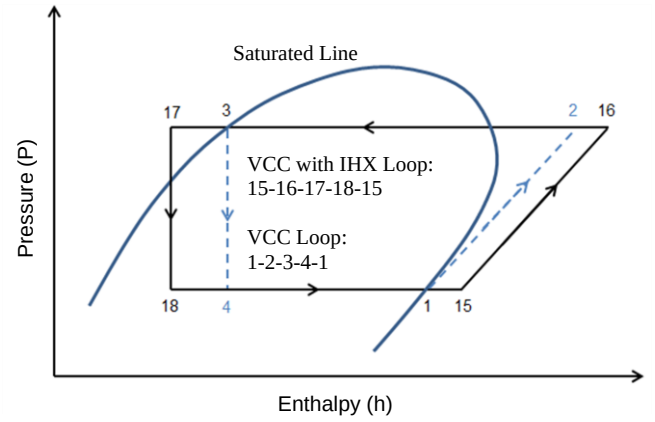

Fig. 4. P-h diagram of the standard VCC with IHX

B. *Internal Heat Exchanger*

One of the concerns in the compressor is having liquid-gas mixture entering it. It is very much unwanted because liquid is incompressible and it can possibly damage the valves or cylinder head of the compressor. Meanwhile, for the expansion device, liquid-gas mixture may enter instead of being subcooled or saturated liquid. This may lead to unwanted phenomena and also lowers the system's performance. Evaporators and condensers are often oversized to ensure that the refrigerant that exits them are vapor and liquid, respectively.

Another solution would be the addition of an internal heat exchanger (IHX) in the system. The common configuration of IHX in refrigeration systems is that the refrigerant in the suction line is being superheated by absorbing heat from the refrigerant that exits the condenser. The schematic and P-h diagrams for standard VCC with IHX are shown in Fig. 3 and Fig. 4, respectively, and for CDERC with IHX are shown in Fig. 5 and Fig. 6, respectively.

Based on the figures shown, the internal heat exchanger increases the refrigerating capacity of the VCC and CDERC when added to the systems. However, one of its drawbacks is the increase of the compressor work [3]. It should also be noted that in CDERC with IHX, the separator temperature and pressure are lower than those of the system without it.

One measure of performance of an internal heat exchanger is the heat transfer ratio (HTR). It is the ratio of the heat absorbed by the cooler fluid from the hotter fluid. As the degree of subcooling increases, the degree of superheating of the vapor in the suction line also increases.

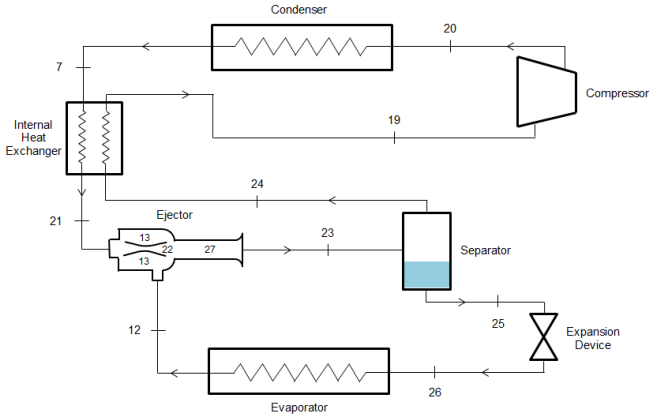

Fig. 5. Schematic diagram of the CDERC with IHX

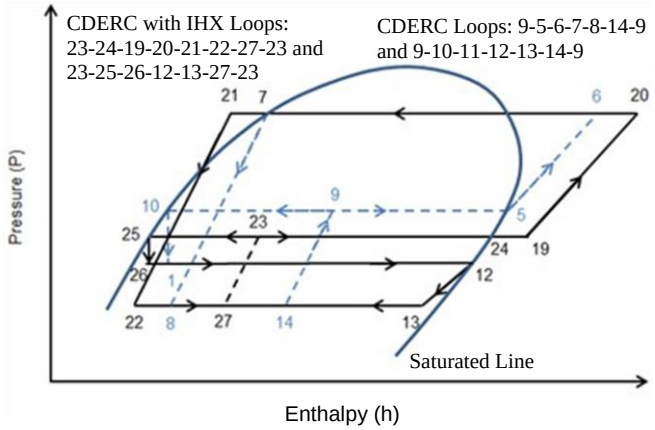

Fig. 6. P-h diagram of the CDERC with IHX

C. *Objectives of the study*

The objective of this paper is to analyze the effects in the system's performance of VCC and CDERC by varying the degree of subcooling and the heat transfer ratio of the internal heat exchanger. Also, the performance of four refrigerants: ammonia, R22, R134a and propane, is observed in both VCC and CDERC with IHX.

II. THEORY AND METHODOLOGY

The analyses for the ejector are patterned from modelling of ejector as used in compressor-driven ejector refrigeration system in our past studies [4-6].

ISBN: 978-988-14048-3-1
ISSN: 2078-0958 (Print); ISSN: 2078-0966 (Online)

A. Governing Equations for the Two-Phase Flow

For this paper, the two-phase flow within the system is assumed to be homogenous and is limited to one-dimensional flow. The refrigerant undergoes a steady-state flow; thus, we have the following equations:

$$\dot{m}_1 = \dot{m}_2 \tag{1}$$

$$\frac{u_1 A_1}{v_1} = \frac{u_2 A_2}{v_2} \tag{2}$$

$$\frac{u_1 A_1}{v_{f1} + x_1 v_{fg1}} = \frac{u_2 A_2}{v_{f2} + x_2 v_{fg2}} \tag{3}$$

Since the ejector is placed horizontally, it is assumed that the effect of gravity is neglected. Modelling that the process is adiabatic, the energy equation for two-phase flow is then

$$\left(h_{f1} + x_1 h_{fg1}\right) + \frac{u_1^2}{2} = \left(h_{f2} + x_2 h_{fg2}\right) + \frac{u_2^2}{2} \tag{4}$$

For the momentum equation, the friction factor f is incorporated and is based on the refrigerant's Reynolds number *Re* [4, 5].

$$-v\frac{dP}{dz} = \frac{d}{dz}\left(\frac{u^2}{2}\right) + 2f\frac{u^2}{D} \tag{5}$$

Moreover, Blasius-type friction type was used in the analyses and has the form [4-6]

$$f = CRe^{-n} \tag{6}$$

where C = 0.118 (constant coefficient) [7]
n = 0.165 (Blasius index) [7]

The Reynolds number is given as

$$Re = uD/v\mu \tag{7}$$

For two-phase flow, the Reynolds number is modified as

$$Re = \frac{uD}{\left(v_f + xv_{fg}\right)\left(\mu_f + x\mu_{fg}\right)} \tag{8}$$

B. Ejector Parts Analyses

The main parts of the ejector are modelled using the governing equations previously discussed. Specific numerical implementations are explained.

Nozzle

In this study, the refrigerant can also enter the ejector as subcooled liquid instead of saturated liquid as in our previous study [6]. For the subcooled region, it is assumed to be isentropic in the current study.

The equations for conservation of mass, momentum and energy were used to simulate the changes in properties of the flow and determine the difference in cross-sectional area along the length of the nozzle.

Shown in Fig. 7 are the thermodynamic states at the inlet of each discrete section of the nozzle (state 1). The thermodynamic state of the section outlet (state 2) will be initially guessed; and the unknown thermodynamic properties are determined through REFPROP [8]. The physical parameters including velocity and geometry will be determined using the equations for conservation of mass and energy given by (3) and (4), respectively.

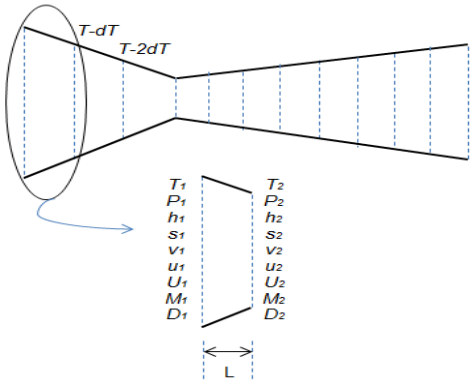

Fig. 7. Discretized sections of nozzle with corresponding thermodynamic values

From the conservation of energy equation given in (4), the velocity at the outlet can be solved as

$$u_2 = \sqrt{2(h_1 - h_2)} \tag{9}$$

The diameter at the outlet D_2 can be solved using the area of the outlet A_2 obtained through the equation for conservation of mass (3). Then, the length of the section is calculated using

$$L = \frac{D_1\left(1 - \sqrt{\left(\frac{u_1}{u_2}\right)\left(\frac{v_2}{v_1}\right)}\right)}{2tan\theta_c} \tag{10}$$

The calculated parameters will be used to check if the momentum equation (5) is satisfied. Since the unknown variables are computed using equations for conservation of mass and energy, satisfying the equation for conservation of momentum by an outlet condition means that convergence with the three governing equations is satisfied. Iteration along constant pressure line for the outlet is done to find the condition that converges with the governing equations. Once convergence in the outlet of a current discrete section is satisfied, another set decrement of temperature is applied to calculate for the adjacent section. The calculated outlet of the current section will then become the inlet of the next.

Piecewise iteration is done until the set outlet pressure of the nozzle is reached. In this process, the iteration for the converging section in the subsonic flow is done until the throat of the nozzle, where the flow will become sonic, is reached; then, the iteration continues for the diverging section in the supersonic flow. In the diverging section, the following equation for piecewise length is used.

$$L = \frac{D_1\left(\sqrt{\left(\frac{u_1}{u_2}\right)\left(\frac{v_2}{v_1}\right)} - 1\right)}{2tan\theta_c} \tag{11}$$

Pre-Mixing Section

For the primary and secondary fluid to be fully mixed, the two fluids must overcome a shear boundary layer due to the difference in velocities and pressures. The primary fluid has higher velocity and relatively low pressure as it exits the

ISBN: 978-988-14048-3-1
ISSN: 2078-0958 (Print); ISSN: 2078-0966 (Online)

converging-diverging nozzle, while the secondary fluid has a subsonic velocity. The condition for mixing is for the two fluids to achieve the same pressure and for the secondary flow to achieve Mach 1.

The diverging stream from the primary flow should be opposed by a converging stream from the secondary flow. This will also accelerate the secondary fluid to achieve sonic flow [9, 10]. The way of solving for this section is the same as that of the converging part of the nozzle, thus equations (1) to (10) are applicable.

The equation for the length of the converging pre-mixing section will be generalized as

$$L = \frac{D_1\left(1-\sqrt{\left(\frac{u_1}{u_2}\right)\left(\frac{v_2}{v_1}\right)}\right)}{2tan\theta_{se}} \quad (12)$$

The iteration will stop if the two fluid flows have the same pressure and if the secondary flow achieves a sonic velocity. Henceforth, it is assumed that the two fluids are fully mixed and satisfying the conservation equations is still used as the convergence criterion for the iteration.

Mixing Section

For the mixing section, the assumption is that the system is not experiencing shock [4, 5; therefore, good choices of angles from ASHRAE [11], ESDU [12] and our previous studies [5, 6] are needed. For this paper, it is assumed that

$$L_m = 3D_m \quad (13)$$

Diffuser

The completely mixed fluid at the end of the mixing section will now flow through the diffuser where its pressure will be elevated but should not reach the superheated state. The velocity of the fluid will decrease throughout the end of the diffuser. The angle range for the diffuser is also based from ASHRAE [11], ESDU [12] and our previous studies [5, 6]. For the diffuser, the equations used for converging section can also be used, but the temperature will be constantly incremented to correspond to pressurization. By applying the conservation of mass and energy and the geometry equations, the length can be computed as:

$$L = \frac{D_1\left(\sqrt{\left(\frac{u_1}{u_2}\right)\left(\frac{v_2}{v_1}\right)}-1\right)}{2tan\theta_c} \quad (14)$$

The convergence criterion discussed is also used. One of the stopping conditions for the diffuser is to achieve a velocity less than 20 m/s at the outlet based on ASHRAE [11], but in the modelling, we force the velocity to achieve 0 m/s to use all the kinetic energy available in the flow. The outlet quality of the fluid at the diffuser outlet should also be checked. Referring to Fig. 6, it should follow the condition

$$x_{9\ or\ 23} = \frac{1}{1+\omega} \quad (15)$$

ω is the entrainment ratio which is the ratio of the mass flow rate of the secondary flow to that of the primary flow.

C. Heat Transfer Ratio in the Internal Heat Exchanger

The degree of superheating will depend on the degree of subcooling and heat transfer ratio which is the ratio of the heat absorbed during superheating to the heat released during subcooling of the refrigerant. Based on Fig. 4 and Fig. 6, the equations for the heat transfer ratios for VCC and CDERC with IHX are as follows:

$$HTR_{VCC,IHX} = \frac{h_{15}-h_1}{h_3-h_{17}} \quad (16)$$

$$HTR_{CDERC,IHX} = \frac{h_{19}-h_{24}}{h_7-h_{21}} \quad (17)$$

D. Coefficient of Performance

The coefficient of performance (COP) is used as a measure of the refrigerating system's performance. It is defined as the ratio of the refrigerating capacity to the compressor work.

For a standard VCC with and without IHX in Fig. 4,

$$COP_{VCC} = \frac{h_1-h_4}{h_2-h_1} \quad (18)$$

$$COP_{VCC,IHX} = \frac{h_1-h_4}{h_{16}-h_{15}} \quad (19)$$

Incorporating the entrainment ratio ω, the COP of CDERC with and without IHX can be expressed as

$$COP_{CDERC} = \omega\frac{(h_{12}-h_{11})}{(h_6-h_5)} \quad (20)$$

$$COP_{CDERC,IHX} = \omega\frac{(h_{12}-h_{26})}{(h_{20}-h_{19})} \quad (21)$$

TABLE I
SYSTEM PERFORMANCE OF THE FOUR REFRIGERANTS IN A STANDARD VCC

Refrigerant	Refrigerating Capacity (kJ/kg)	Specific Compressor Work (kJ/kg)	COP
Ammonia	1066.01	215.50	4.95
R22	153.51	32.36	4.74
R134a	139.25	29.75	4.68
Propane	262.15	56.97	4.60

TABLE II
SYSTEM PERFORMANCE OF THE FOUR REFRIGERANTS IN CDERC

Refrigerant	Refrigerating Capacity (kJ/kg)	Specific Compressor Work (kJ/kg)	COP
Ammonia	1262.66	192.80	5.57
R22	200.10	25.84	6.04
R134a	191.75	23.69	6.07
Propane	357.97	43.17	6.22

III. RESULTS AND DISCUSSION

The independent parameters for this study are the evaporating and condensing temperatures, which are set at -5°C and 40°C, respectively. The degree of subcooling is varied from 0 to 10°C, with one degree increment. Moreover, the HTR is varied from 0 to 1, with 0.10 increments.

Another interest in this study is the performance of the four refrigerants which are ammonia, R22, R134a and propane in VCC and CDERC with IHX.

ISBN: 978-988-14048-3-1
ISSN: 2078-0958 (Print); ISSN: 2078-0966 (Online)

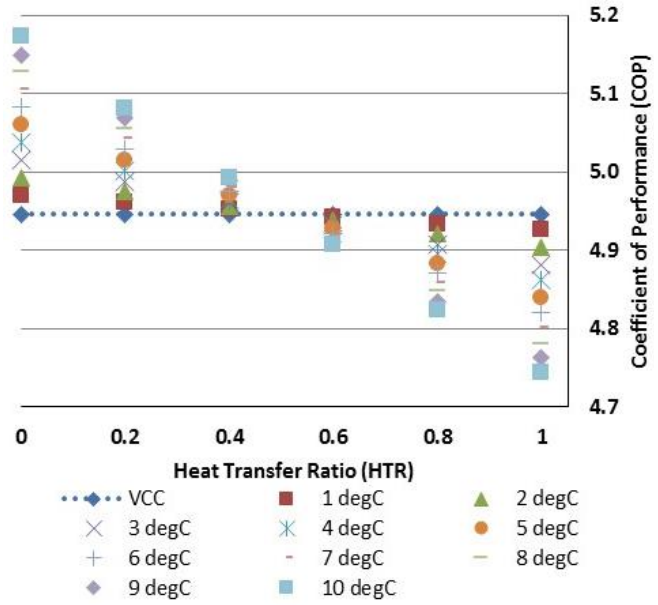

Fig. 8. System Performance of VCC with IHX Using Ammonia as Refrigerant

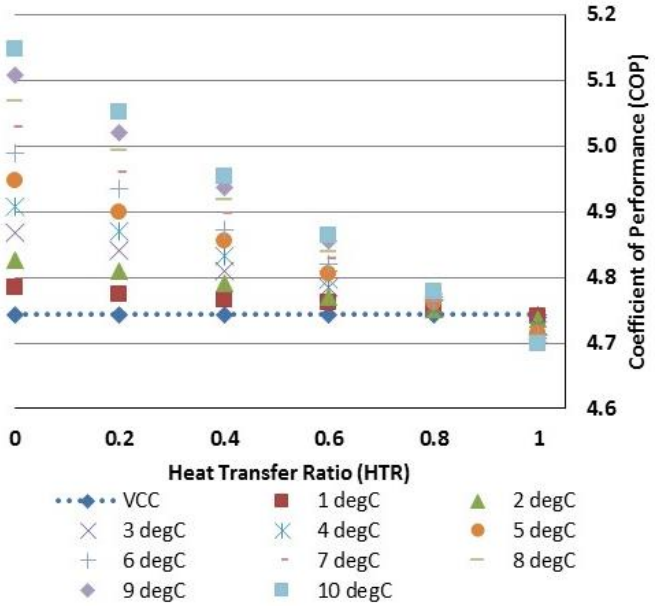

Fig. 9. System Performance of VCC with IHX Using R22 as Refrigerant

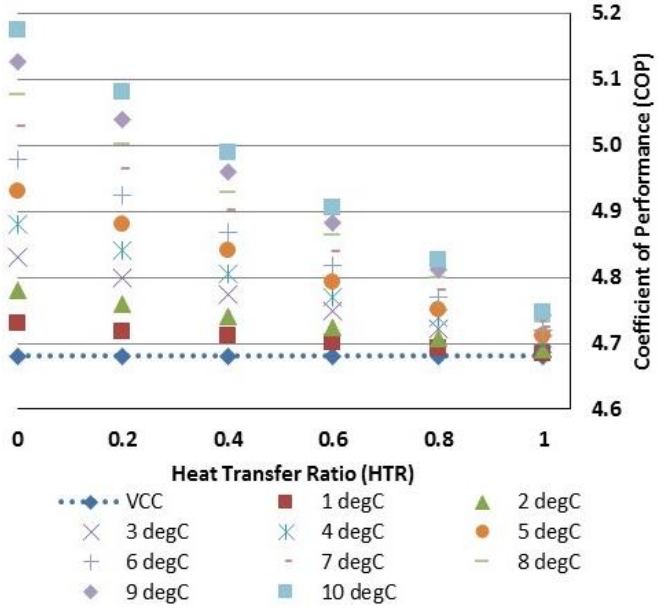

Fig. 10. System Performance of VCC with IHX Using R134a as Refrigerant

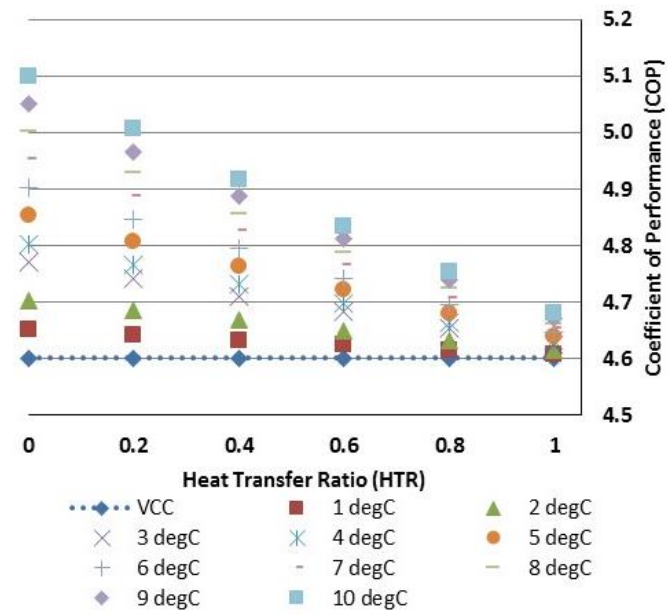

Fig. 11. System Performance of VCC with IHX Using Propane as Refrigerant

A. Performance of Standard Vapor Compression Cycle and Compressor-Driven Ejector Refrigeration Cycle

The cycles being studied on will be the benchmark to determine if introducing an internal heat exchanger would improve the system's performance.

Table I and Table II show the COP of the four refrigerants for the standard VCC and CDERC.

Comparing the COPs of VCC and CDERC, it is clearly seen that CDERC is better. In CDERC, the refrigerating capacity is increased and the specific work is significantly decreased.

B. Vapor Compression Cycle with Internal Heat Exchanger

Fig. 8 to Fig. 11 show the COP versus HTR graph of the four refrigerants with various values of degree of subcooling. Trend lines of the COP for VCC are added in the graph to easily compare the performance of the system with and without the IHX.

The COP of the system increases with the degree of subcooling. However, it decreases as HTR increases. The COP of the system with higher degree of subcooling rapidly drops as HTR increases compared with those lower values of subcooling.

Among the four refrigerants, the performance of systems that use R134a and propane are improved with the addition of internal heat exchanger. However, the system that uses ammonia has better performance, with subcooling ranges from 0 to 10°C, if its HTR is less than 0.50. For R22, it performs better if its HTR is limited up to 0.80. The temperature of ammonia and R22 increase quickly compared to R134a and propane. This results to higher inlet temperature of the vapor at the compressor. Thus, making the vapor denser and increasing the compressor work. On this basis, Ammonia and R22 are not advisable for IHX as the reliability may be compromised by higher temperature.

ISBN: 978-988-14048-3-1
ISSN: 2078-0958 (Print); ISSN: 2078-0966 (Online)

C. Compressor-Driven Ejector Refrigeration Cycle with Internal Heat Exchanger

Fig. 12 shows the COP versus HTR graph of propane with various degree of subcooling. Trend line of the COP for CDERC without IHX is added to easily compare the performance of all the systems with and without IHX. The three other refrigerants do not show improvement in COP by adding IHX in the CDERC, so they are not shown here anymore. Propane could operate up to 4°C subcooling with 0.5 HTR, outperforming CDERC without IHX.

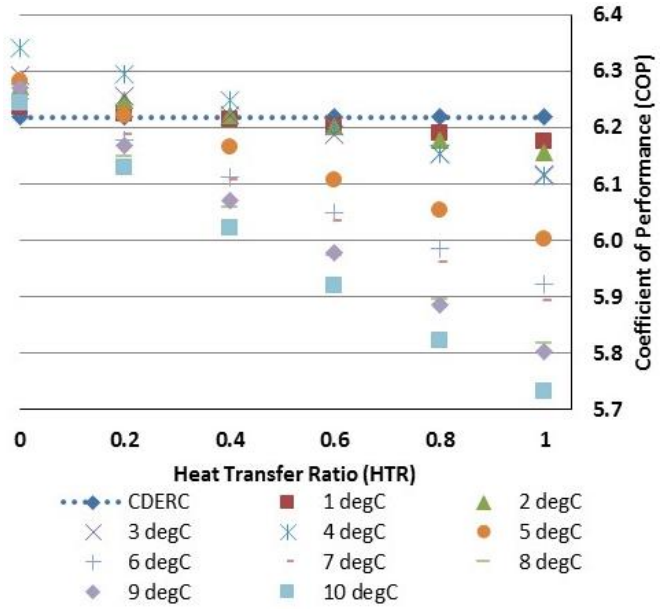

Fig. 12. System Performance of CDERC with IHX Using Propane as Refrigerant

IV. Conclusion

A theoretical analysis on the effect of internal heat exchanger (IHX) on a system using standard vapor compression cycle (VCC) and compressor-driven ejector refrigeration cycle (CDERC) is conducted. Parameters such as the degree of subcooling of the refrigerant at the condenser exit and the heat transfer ratio (HTR) in the IHX are varied while the condensing and evaporating temperatures are held constant. In both VCC and CDERC with IHX, the refrigerating capacity is not only increased but also results to higher compressor work.

VCC with IHX using R134a and propane have higher COPs, with degree of subcooling up to 10°C and HTR up to 1, compared to a system without it. For ammonia and R22, limiting HTRs of 0.50 and 0.80, respectively, indicate that IHX can compromise reliability of those systems.

For the CDERC with IHX, only propane shows satisfactory result. It is not advisable to use ammonia in this kind of system because it has lower COP in this case.

Adding internal heat exchanger in a compressor-driven refrigeration cycle does not necessarily improve the system. The IHX mainly functions as a safeguard to ensure that the fluid that enters the compressor is in vapor form. In some conditions, like for R134a, the IHX improves the COP.

Nomenclature

A	cross sectional area	(m^2)
C	Blasius friction-type factor coefficient	(-)
COP	coefficient of performance	(-)
D	hydraulic diameter	(m)
f	homogeneous friction factor	(-)
h	enthalpy	(J/kg)
HTR	heat transfer ratio	(-)
L	length	(m)
$\dot{m}$	mass flow rate	(kg/s)
n	Blasius index	(-)
P	pressure	(Pa)
Re	Reynolds number	(-)
u	velocity	(m/s)
v	specific volume	(m^3/kg)
x	quality	(-)
z	flow axis	(m)
θ	angle	(°)
μ	viscosity	(Pa-s)
ω	entrainment ratio	(-)
Subscripts		
1-27	state points	

Acknowledgment

The authors are sincerely thankful to the Engineering Research and Development for Technology (ERDT) Program of the Department of Science and Technology – Science Education Institute (DOST – SEI) of the Republic of the Philippines for funding the dissemination of this research.

References

[1] Aleph Zero – Refrigeration [Online] http://www.alephzero.co.uk/ref/vapcomcyc.htm.
[2] K. Sumeru, H. Nasution, F. N. Ani, (2012) A Review on Two-Phase Ejector as an Expansion Device in Vapor Compression Refrigeration Cycle, Renewable and Sustainable Energy Reviews, 4927-4937.
[3] F. J. Antonio, M. S. Berana and L. A. M. Danao, Design of a Screw Heat Exchanger as the Liquid-Suction Heat Exchanger in a Vapor Compression Refrigeration System, Proceedings of the ASME 2015 International Mechanical Engineering Congress and Exposition (IMECE2015), Houston, Texas, USA, November 13-19, 2015.
[4] M. S. Berana and G. D. Espena, Modelling of Ejector Refrigeration System and Its Application to the Design of an Ejector Cooler for a Hot-Spring Resort in the Philippines, Proceedings of the World Congress on Engineering - The 2016 International Conference of Mechanical Engineering, Imperial College, London, United Kingdom, June 29–July 1, 2016.
[5] B. E.Abuan and M. S. Berana, Ejector Profile Modelling for Heat-Driven Ejector Refrigeration System without Involving Shock, Proceedings of the ASME 2015 International Mechanical Engineering Congress and Exposition (IMECE2015), Houston, Texas, USA, November 13-19, 2015.
[6] J.C.S. Garcia, J.Y.T. Alcaraz, J.R.A. Alvarez, B.E. Abuan, M.S. Berana, (2014) Ejector Profile Modelling for Compressor-Driven Ejector Refrigeration System, Philippine Engineering Journal, XXXV (2), 38-56.
[7] D.D. Joseph, B.H. Yang, (2010). Friction factor correlations for laminar, transition and turbulent flow in smooth pipes. Physica D: Nonlinear Phenomena, Vol. 239, 1318-1328.
[8] E. W. Lemmon, M. O. McLinden, M. L. Huber, NIST Standard Reference Database 23: Reference Fluid Thermodynamic and Transport Properties-REFPROP, Version 9.1, National Institute of Standards and Technology (NIST), Gaithersburg, Maryland, 2013
[9] E.T. Bermido, Ejector Design for Powerplant Application, University of the Philippines Diliman, May 2012.
[10] S.Aphornratana, I.W. Eames (1997). A small capacity steam-ejector refrigerator: experimental investigation of a system using ejector with movable primary nozzle. International Journal of Refrigeration, Vol. 20, 352-358.
[11] ASHRAE, 1979. Steam-Jet Refrigeration Equipment, Equipment Handbook, vol.13, pp. 13.1-13.6.
[12] ESDU, 1986. Ejectors and Jet Pumps, Design for Steam Driven Flow, Engineering Science Data item 86030, Engineering Science Data Unit, London.